

Local discontinuous Galerkin method for surface diffusion and Willmore flow of graphs

Yan Xu* and Chi-Wang Shu †

Abstract

In this paper, we develop a local discontinuous Galerkin (LDG) finite element method for surface diffusion and Willmore flow of graphs. We prove L^2 stability for the equation of surface diffusion of graphs and energy stability for the equation of Willmore flow of graphs. We provide numerical simulation results for different types of solutions of these two types of the equations to illustrate the accuracy and capability of the LDG method.

AMS subject classification: 65M60, 35K55

Key words: local discontinuous Galerkin method, surface diffusion of graphs, Willmore flow of graphs, stability

*Department of Mathematics, University of Science and Technology of China, Hefei, Anhui 230026, P.R. China. Email: yxu@ustc.edu.cn. Research supported by NSFC grant 10601055 and Foundation for Authors of Excellent Doctoral Dissertations of the Chinese Academy of Sciences.

†Division of Applied Mathematics, Brown University, Providence, RI 02912, USA. E-mail: shu@dam.brown.edu. The research of this author is supported in part by NSFC grant 10671190 during his visit to the Department of Mathematics, University of Science and Technology of China, Hefei, Anhui 230026, P.R. China. Additional support is provided by NSF grant DMS-0510345.

1 Introduction

In this paper, we consider the surface diffusion of graphs

$$u_t + \nabla \cdot \left(Q \left(\mathbf{I} - \frac{\nabla u \otimes \nabla u}{Q^2} \right) \nabla H \right) = 0 \quad (1.1)$$

and the equation of Willmore flow of graphs

$$u_t + Q \nabla \cdot \left(\frac{1}{Q} \left(\mathbf{I} - \frac{\nabla u \otimes \nabla u}{Q^2} \right) \nabla(QH) \right) - \frac{1}{2} Q \nabla \cdot \left(\frac{H^2}{Q} \nabla u \right) = 0, \quad (1.2)$$

where Q is the area element

$$Q = \sqrt{1 + |\nabla u|^2} \quad (1.3)$$

and H is mean curvature of the domain boundary Γ

$$H = \nabla \cdot \left(\frac{\nabla u}{Q} \right). \quad (1.4)$$

These two equations are both highly nonlinear fourth-order PDEs.

The surface diffusion equation [14]

$$V = \Delta_\Gamma H \quad \text{on } \Gamma \quad (1.5)$$

models the diffusion of mass within the bounding surface of a solid body, where V is the normal velocity of the evolving surface Γ ,

$$V = -\frac{u_t}{Q(u)}, \quad (1.6)$$

and Δ_Γ denotes the Laplace-Beltrami operator

$$\Delta_\Gamma v = \frac{1}{Q(u)} \nabla \cdot \left(Q(u) \left(\mathbf{I} - \frac{\nabla u \otimes \nabla u}{Q(u)^2} \right) \nabla v \right). \quad (1.7)$$

Equation (1.5) is described as a mechanism of surface formation under the action of chemical potential. For a surface with constant surface energy density, the appropriate chemical potential in this setting is the mean curvature H . In [19], the authors describe an algorithm for the evolution of elastic curves. Some interesting computational results have been collected in [1, 3, 19, 14]. In [3], A finite difference scheme was discussed for the

surface diffusion of graphs. A space-time finite element method for axially symmetric surfaces is presented by Coleman, Falk and Moakher in [12]. In [1], Bänsch, Morin and Nchetto presented a variational formulation for graphs and derived a priori error estimates for a semi-discrete finite element discretization. Deckelnick, Dziuk and Elliott provided an error analysis [14] for the anisotropic case.

A similar evolution law is the Willmore flow

$$V = \Delta_{\Gamma} H + \frac{1}{2} H^3 - 2HK, \quad (1.8)$$

where K is the Gauss curvature of Γ . The Willmore flow is an evolutionary law for minimizing mean curvature of curves or surfaces. In [15], an implicit numerical scheme for the Willmore flow of graphs based on a finite element method together with its numerical analysis is presented. A level set formulation for the Willmore flow can be found in [16]. Asymptotical convergence of the phase-field model for the Willmore flow was proved and numerical simulations were performed by finite difference methods in [17, 18]. A finite difference scheme for the Willmore flow of graphs was discussed in [21].

In this paper we pay particular attention to the discontinuous finite element method, specifically, to the local discontinuous Galerkin (LDG) method. The considered LDG method is a particular version of the discontinuous Galerkin (DG) method, which uses a completely discontinuous piecewise polynomial space for the numerical solution and the test functions. It was first designed as a method for solving hyperbolic conservation laws containing only first order spatial derivatives, e.g. Reed and Hill [20] for solving linear equations, and Cockburn et al. [7, 6, 5, 8] for solving nonlinear hyperbolic equations.

Later, the LDG method was introduced by Cockburn and Shu in [9] as an extension of the Runge-Kutta DG (RKDG) method to general convection-diffusion problems, and of the DG scheme for the compressible Navier-Stokes equations proposed by Bassi and Rebay in [2]. More general information about DG methods for elliptic and hyperbolic partial differential equations can be found in [4, 10, 11, 13]. Recently, the LDG techniques have been developed for various nonlinear wave equations with high order derivatives [26, 24, 25]. In [22, 23], the LDG methods with provable energy stability were designed for the Cahn-Hilliard equations and the Allen-Cahn/Cahn-Hilliard system

which are also nonlinear fourth-order equations.

The DG method possesses several properties to make it very attractive for practical computations, such as easy parallelization, easy adaptivity, and simple treatment of boundary conditions. The most important property of this method is its strong stability and high-order accuracy. All of these good properties motivate us to develop the LDG method for the curvature flow problems.

The paper is organized as follows. In Section 2, we present and analyze our LDG method for the surface diffusion of graphs equation (1.1). The details of the LDG method and the proof of the L^2 stability are described. In Section 3, we present the LDG method for the Willmore flow of graphs equation (1.2). We give a proof of the energy stability in Section 3.2. Section 4 contains numerical results for the nonlinear problems which include the surface diffusion of graphs and Willmore flow of graphs. These numerical results demonstrate the accuracy and capability of the LDG methods. Concluding remarks are given in Section 5.

2 The LDG method for the surface diffusion of graphs

In this section, we consider the local discontinuous Galerkin method for the surface diffusion of graphs equation (1.1) in $\Omega \in \mathbb{R}^d$ with $d \leq 3$. Although we do not address numerical results in three dimensions in this paper, the LDG methods and the stability results of this paper are valid for all $d \leq 3$.

2.1 Notation

Let \mathcal{T}_h denote a tessellation of Ω with shape-regular elements K . Let Γ denote the union of the boundary faces of elements $K \in \mathcal{T}_h$, i.e. $\Gamma = \cup_{K \in \mathcal{T}_h} \partial K$, and $\Gamma_0 = \Gamma \setminus \partial\Omega$.

In order to describe the flux functions we need to introduce some notations. Let e be a face shared by the “left” and “right” elements K_L and K_R (we refer to [26] and [22] for a proper definition of “left” and “right” in our context). Define the normal vectors ν_L and ν_R on e pointing exterior to K_L and K_R , respectively. If ψ is a function on

K_L and K_R , but possibly discontinuous across e , let ψ_L denote $(\psi|_{K_L})|_e$ and ψ_R denote $(\psi|_{K_R})|_e$, the left and right trace, respectively.

Let $\mathcal{P}^p(K)$ be the space of polynomials of degree at most $p \geq 0$ on $K \in \mathcal{T}_h$. The finite element spaces are denoted by

$$V_h = \left\{ \varphi : \varphi|_K \in \mathcal{P}^p(K), \quad \forall K \in \mathcal{T}_h \right\},$$

$$\Sigma_h = \left\{ \boldsymbol{\eta} = (\eta_1, \dots, \eta_d)^T : \eta_l|_K \in \mathcal{P}^p(K), \quad l = 1 \dots d, \quad \forall K \in \mathcal{T}_h \right\}.$$

Note that functions in V_h and Σ_h are allowed to have discontinuities across element interfaces.

Here we only consider the periodic boundary conditions. Notice that the assumption of periodic boundary conditions is for simplicity only and is not essential: the method can be easily designed for non-periodic boundary conditions. The development of the LDG method for the non-periodic boundary conditions can be found in [22, 23].

2.2 The LDG method

To define the local discontinuous Galerkin method, we further rewrite the equation (1.1) as a first order system:

$$u_t + \nabla \cdot \mathbf{s} = 0, \tag{2.1a}$$

$$\mathbf{s} - \mathbf{E}(\mathbf{r})\mathbf{p} = 0, \tag{2.1b}$$

$$\mathbf{p} - \nabla H = 0, \tag{2.1c}$$

$$H - \nabla \cdot \mathbf{q} = 0, \tag{2.1d}$$

$$\mathbf{q} - \frac{\mathbf{r}}{Q} = 0, \tag{2.1e}$$

$$\mathbf{r} - \nabla u = 0, \tag{2.1f}$$

with

$$\mathbf{E}(\mathbf{r}) = Q \left(\mathbf{I} - \frac{\mathbf{r} \otimes \mathbf{r}}{Q^2} \right), \tag{2.2}$$

$$Q = \sqrt{1 + |\mathbf{r}|^2}, \tag{2.3}$$

where $u, H, Q \in L^2(\Omega)$, $\mathbf{s}, \mathbf{p}, \mathbf{q}, \mathbf{r} \in (L^2(\Omega))^d$, $\mathbf{E}(\mathbf{r}), \mathbf{I} \in (L^2(\Omega))^d \times (L^2(\Omega))^d$ and \mathbf{I} is the $d \times d$ identity matrix.

Applying the LDG method to the system (2.1), we have the scheme: Find $u, H \in V_h$, $\mathbf{s}, \mathbf{p}, \mathbf{q}, \mathbf{r} \in \Sigma_h$, such that, for all test function $\varphi, \vartheta \in V_h$ and $\phi, \boldsymbol{\eta}, \boldsymbol{\rho}, \boldsymbol{\zeta} \in \Sigma_h$, we have

$$\int_K u_t \varphi dK - \int_K \mathbf{s} \cdot \nabla \varphi dK + \int_{\partial K} \widehat{\mathbf{s}} \cdot \boldsymbol{\nu} \varphi ds = 0, \quad (2.4a)$$

$$\int_K \mathbf{s} \cdot \phi dK - \int_K \mathbf{E}(\mathbf{r}) \mathbf{p} \cdot \phi dK = 0, \quad (2.4b)$$

$$\int_K \mathbf{p} \cdot \boldsymbol{\eta} dK + \int_K H \nabla \cdot \boldsymbol{\eta} dK - \int_{\partial K} \widehat{H} \boldsymbol{\nu} \cdot \boldsymbol{\eta} ds = 0, \quad (2.4c)$$

$$\int_K H \vartheta dK + \int_K \mathbf{q} \cdot \nabla \vartheta dK - \int_{\partial K} \widehat{\mathbf{q}} \cdot \boldsymbol{\nu} \vartheta ds = 0, \quad (2.4d)$$

$$\int_K \mathbf{q} \cdot \boldsymbol{\rho} dK - \int_K \frac{\mathbf{r}}{Q} \cdot \boldsymbol{\rho} dK = 0, \quad (2.4e)$$

$$\int_K \mathbf{r} \cdot \boldsymbol{\zeta} dK + \int_K u \nabla \cdot \boldsymbol{\zeta} dK - \int_{\partial K} \widehat{u} \boldsymbol{\nu} \cdot \boldsymbol{\zeta} ds = 0, \quad (2.4f)$$

where $\mathbf{E}(\mathbf{r})$ and Q are computed by (2.2) and (2.3).

The ‘‘hat’’ terms in (2.4) in the cell boundary terms from integration by parts are the so-called ‘‘numerical fluxes’’, which are functions defined on the cell edges and should be designed based on different guiding principles for different PDEs to ensure stability. It turns out that we can take the simple choices such that

$$\widehat{\mathbf{s}}|_e = \mathbf{s}_L, \quad \widehat{\mathbf{q}}|_e = \mathbf{q}_R, \quad \widehat{H}|_e = H_L, \quad \widehat{u}|_e = u_R. \quad (2.5)$$

2.3 L^2 stability

In this section, we prove the L^2 stability of the LDG method for the surface diffusion of graphs defined in the previous section.

Proposition 2.1. (*L^2 stability*) *The solution of the surface diffusion of graphs to the schemes (2.4)-(2.5) satisfies the L^2 stability*

$$\frac{1}{2} \frac{d}{dt} \int_{\Omega} u^2 d\Omega + \int_{\Omega} H^2 d\Omega = 0. \quad (2.6)$$

Proof. We take the test functions

$$\varphi = u, \quad \phi = \mathbf{r}, \quad \boldsymbol{\eta} = \mathbf{q}, \quad \vartheta = H, \quad \boldsymbol{\rho} = -\mathbf{p}, \quad \boldsymbol{\zeta} = -\mathbf{s}.$$

Then we have

$$\int_K u_t u dK - \int_K \mathbf{s} \cdot \nabla u dK + \int_{\partial K} \widehat{\mathbf{s}} \cdot \boldsymbol{\nu} u ds = 0, \quad (2.7a)$$

$$\int_K \mathbf{s} \cdot \mathbf{r} dK - \int_K \mathbf{E}(\mathbf{r}) \mathbf{p} \cdot \mathbf{r} dK = 0, \quad (2.7b)$$

$$\int_K \mathbf{p} \cdot \mathbf{q} dK + \int_K H \nabla \cdot \mathbf{q} dK - \int_{\partial K} \widehat{H} \boldsymbol{\nu} \cdot \mathbf{q} ds = 0, \quad (2.7c)$$

$$\int_K H^2 dK + \int_K \mathbf{q} \cdot \nabla H dK - \int_{\partial K} \widehat{\mathbf{q}} \cdot \boldsymbol{\nu} H ds = 0, \quad (2.7d)$$

$$- \int_K \mathbf{q} \cdot \mathbf{p} dK + \int_K \frac{\mathbf{r}}{Q} \cdot \mathbf{p} dK = 0, \quad (2.7e)$$

$$- \int_K \mathbf{r} \cdot \mathbf{s} dK - \int_K u \nabla \cdot \mathbf{s} dK + \int_{\partial K} \widehat{u} \boldsymbol{\nu} \cdot \mathbf{s} ds = 0. \quad (2.7f)$$

Summing up the equations (2.7a)-(2.7f), we obtain

$$\begin{aligned} & \int_K u_t u dK + \int_K H^2 dK + \int_K \left(\frac{\mathbf{r}}{Q} \right) \cdot \mathbf{p} dK - \int_K (\mathbf{E}(\mathbf{r}) \mathbf{p}) \cdot \mathbf{r} dK \\ & - \int_K \nabla \cdot (\mathbf{s} u) + \int_{\partial K} \widehat{\mathbf{s}} \cdot \boldsymbol{\nu} u ds + \int_{\partial K} \widehat{u} \boldsymbol{\nu} \cdot \mathbf{s} ds \\ & + \int_K \nabla \cdot (\mathbf{q} H) dK - \int_{\partial K} \widehat{\mathbf{q}} \cdot \boldsymbol{\nu} H ds - \int_{\partial K} \widehat{H} \boldsymbol{\nu} \cdot \mathbf{q} ds = 0. \end{aligned}$$

Using the relation

$$Q^2 = 1 + |\mathbf{r}|^2, \quad \left(\frac{\mathbf{r}}{Q} \right) \cdot \mathbf{p} - (\mathbf{E}(\mathbf{r}) \mathbf{p}) \cdot \mathbf{r} = 0,$$

we have

$$\begin{aligned} & \int_K u_t u dK + \int_K H^2 dK - \int_K \nabla \cdot (\mathbf{s} u) + \int_{\partial K} \widehat{\mathbf{s}} \cdot \boldsymbol{\nu} u ds + \int_{\partial K} \widehat{u} \boldsymbol{\nu} \cdot \mathbf{s} ds \\ & + \int_K \nabla \cdot (\mathbf{q} H) dK - \int_{\partial K} \widehat{\mathbf{q}} \cdot \boldsymbol{\nu} H ds - \int_{\partial K} \widehat{H} \boldsymbol{\nu} \cdot \mathbf{q} ds = 0. \end{aligned}$$

Summing up over all elements K , with the numerical fluxes (2.5) and the periodic boundary conditions, we get

$$\int_{\Omega} u_t u d\Omega + \int_{\Omega} H^2 d\Omega = 0,$$

i.e.

$$\frac{1}{2} \frac{d}{dt} \int_{\Omega} u^2 d\Omega + \int_{\Omega} H^2 d\Omega = 0.$$

□

3 The LDG method for the Willmore flow of graphs

In this section, we consider the local discontinuous Galerkin method for the Willmore flow of graphs equation (1.2) in $\Omega \in \mathbb{R}^d$ with $d \leq 3$.

3.1 The LDG method

To define the local discontinuous Galerkin method, we further rewrite the equation (1.2) as a first order system:

$$\frac{u_t}{Q} + \nabla \cdot (\mathbf{s} - \mathbf{v}) = 0, \quad (3.1a)$$

$$\mathbf{s} - \mathbf{E}(\mathbf{r})\mathbf{p} = 0, \quad (3.1b)$$

$$\mathbf{v} - \frac{1}{2} \frac{H^2}{Q} \mathbf{r} = 0, \quad (3.1c)$$

$$\mathbf{p} - \nabla W = 0, \quad (3.1d)$$

$$W - QH = 0, \quad (3.1e)$$

$$H - \nabla \cdot \mathbf{q} = 0, \quad (3.1f)$$

$$\mathbf{q} - \frac{\mathbf{r}}{Q} = 0, \quad (3.1g)$$

$$\mathbf{r} - \nabla u = 0, \quad (3.1h)$$

with

$$\mathbf{E}(\mathbf{r}) = \frac{1}{Q} \left(\mathbf{I} - \frac{\mathbf{r} \otimes \mathbf{r}}{Q^2} \right), \quad (3.2)$$

$$Q = \sqrt{1 + |\mathbf{r}|^2}, \quad (3.3)$$

where $u, H, W, Q \in L^2(\Omega)$, $\mathbf{s}, \mathbf{v}, \mathbf{p}, \mathbf{q}, \mathbf{r} \in (L^2(\Omega))^d$, $\mathbf{E}(\mathbf{r}), \mathbf{I} \in (L^2(\Omega))^d \times (L^2(\Omega))^d$ and \mathbf{I} is the $d \times d$ identity matrix.

Applying the LDG method to the system (3.1), we have the scheme: Find $u, H, W \in V_h$, $\mathbf{s}, \mathbf{v}, \mathbf{p}, \mathbf{q}, \mathbf{r} \in \Sigma_h$, such that, for all test function $\varphi, \xi, \vartheta \in V_h$ and $\boldsymbol{\phi}, \boldsymbol{\psi}, \boldsymbol{\eta}, \boldsymbol{\rho}, \boldsymbol{\zeta} \in \Sigma_h$, we have

$$\int_K \frac{u_t}{Q} \varphi dK - \int_K (\mathbf{s} - \mathbf{v}) \cdot \nabla \varphi dK + \int_{\partial K} (\widehat{\mathbf{s} \cdot \boldsymbol{\nu}} - \widehat{\mathbf{v} \cdot \boldsymbol{\nu}}) \varphi ds = 0, \quad (3.4a)$$

$$\int_K \mathbf{s} \cdot \boldsymbol{\phi} dK - \int_K \mathbf{E}(\mathbf{r}) \mathbf{p} \cdot \boldsymbol{\phi} dK = 0, \quad (3.4b)$$

$$\int_K \mathbf{v} \cdot \boldsymbol{\psi} dK - \int_K \frac{1}{2} \frac{H^2}{Q} \mathbf{r} \cdot \boldsymbol{\psi} dK = 0, \quad (3.4c)$$

$$\int_K \mathbf{p} \cdot \boldsymbol{\eta} dK + \int_K W \nabla \cdot \boldsymbol{\eta} dK - \int_{\partial K} \widehat{W} \boldsymbol{\nu} \cdot \boldsymbol{\eta} ds = 0, \quad (3.4d)$$

$$\int_K W \xi dK - \int_K Q H \xi dK = 0, \quad (3.4e)$$

$$\int_K H \vartheta dK + \int_K \mathbf{q} \cdot \nabla \vartheta dK - \int_{\partial K} \widehat{\mathbf{q}} \cdot \boldsymbol{\nu} \vartheta ds = 0, \quad (3.4f)$$

$$\int_K \mathbf{q} \cdot \boldsymbol{\rho} dK - \int_K \frac{\mathbf{r}}{Q} \cdot \boldsymbol{\rho} dK = 0, \quad (3.4g)$$

$$\int_K \mathbf{r} \cdot \boldsymbol{\zeta} dK + \int_K u \nabla \cdot \boldsymbol{\zeta} dK - \int_{\partial K} \widehat{u} \boldsymbol{\nu} \cdot \boldsymbol{\zeta} ds = 0, \quad (3.4h)$$

where $\mathbf{E}(\mathbf{r})$ and Q are computed by (3.2) and (3.3).

Similar to the development in [22], it turns out that we can take the simple choices for the numerical fluxes such that

$$\widehat{\mathbf{s}}|_e = \mathbf{s}_L, \quad \widehat{\mathbf{v}}|_e = \mathbf{v}_L, \quad \widehat{\mathbf{q}}|_e = \mathbf{q}_R, \quad \widehat{W}|_e = W_L, \quad \widehat{u}|_e = u_R. \quad (3.5)$$

3.2 Energy stability

In this section, we prove the energy stability of the LDG method for the Willmore flow equation defined in the previous section.

Proposition 3.1. *(Energy stability) The solution of the Willmore flow equation to the schemes (3.4)-(3.5) satisfies the energy stability*

$$\frac{1}{2} \frac{d}{dt} \int_{\Omega} H^2 Q d\Omega + \int_{\Omega} \frac{(u_t)^2}{Q} d\Omega = 0. \quad (3.6)$$

Proof. After taking the time derivative, we choose the test functions $\vartheta = W$, $\boldsymbol{\rho} = -\mathbf{p}$, $\boldsymbol{\zeta} = \mathbf{v} - \mathbf{s}$ in (3.4f), (3.4g) and (3.4h). Then we get

$$\int_K H_t W dK + \int_K \mathbf{q}_t \cdot \nabla W dK - \int_{\partial K} \widehat{\mathbf{q}}_t \cdot \boldsymbol{\nu} W ds = 0, \quad (3.7)$$

$$- \int_K \mathbf{q}_t \cdot \mathbf{p} dK + \int_K \left(\frac{\mathbf{r}}{Q} \right)_t \cdot \mathbf{p} dK = 0, \quad (3.8)$$

$$\int_K \mathbf{r}_t \cdot (\mathbf{v} - \mathbf{s}) dK + \int_K u_t \nabla \cdot (\mathbf{v} - \mathbf{s}) dK - \int_{\partial K} \widehat{u}_t \boldsymbol{\nu} \cdot (\mathbf{v} - \mathbf{s}) ds = 0. \quad (3.9)$$

For (3.4a)-(3.4e), we take the test functions

$$\varphi = u_t, \quad \phi = \mathbf{r}_t, \quad \psi = -\mathbf{r}_t, \quad \eta = \mathbf{q}_t, \quad \xi = -H_t.$$

Then we have

$$\int_K \frac{(u_t)^2}{Q} dK - \int_K (\mathbf{s} - \mathbf{v}) \cdot \nabla u_t dK + \int_{\partial K} (\widehat{\mathbf{s}} \cdot \boldsymbol{\nu} - \widehat{\mathbf{v}} \cdot \boldsymbol{\nu}) u_t ds = 0, \quad (3.10)$$

$$\int_K \mathbf{s} \cdot \mathbf{r}_t dK - \int_K \mathbf{E}(\mathbf{r}) \mathbf{p} \cdot \mathbf{r}_t dK = 0, \quad (3.11)$$

$$- \int_K \mathbf{v} \cdot \mathbf{r}_t dK + \int_K \frac{1}{2} \frac{H^2}{Q} \mathbf{r} \cdot \mathbf{r}_t dK = 0, \quad (3.12)$$

$$\int_K \mathbf{p} \cdot \mathbf{q}_t dK + \int_K W \nabla \cdot \mathbf{q}_t dK - \int_{\partial K} \widehat{W} \boldsymbol{\nu} \cdot \mathbf{q}_t ds = 0, \quad (3.13)$$

$$- \int_K W H_t dK + \int_K Q H H_t dK = 0. \quad (3.14)$$

Summing up the equations (3.7)-(3.14), we obtain

$$\begin{aligned} & \int_K \frac{1}{2} \frac{H^2}{Q} \mathbf{r} \cdot \mathbf{r}_t dK + \int_K Q H H_t dK + \int_K \frac{(u_t)^2}{Q} dK \\ & + \int_K \left(\frac{\mathbf{r}}{Q} \right)_t \cdot \mathbf{p} dK - \int_K \mathbf{E}(\mathbf{r}) \mathbf{p} \cdot \mathbf{r}_t dK \\ & - \int_K \nabla \cdot ((\mathbf{s} - \mathbf{v}) u_t) + \int_{\partial K} (\widehat{\mathbf{s}} \cdot \boldsymbol{\nu} - \widehat{\mathbf{v}} \cdot \boldsymbol{\nu}) u_t ds + \int_{\partial K} \widehat{u}_t \boldsymbol{\nu} \cdot (\mathbf{s} - \mathbf{v}) ds \\ & + \int_K \nabla \cdot (\mathbf{q}_t W) dK - \int_{\partial K} \widehat{\mathbf{q}_t} \cdot \boldsymbol{\nu} W ds - \int_{\partial K} \widehat{W} \boldsymbol{\nu} \cdot \mathbf{q}_t ds = 0. \end{aligned}$$

Using the relation

$$Q_t = \frac{\mathbf{r} \cdot \mathbf{r}_t}{Q}, \quad \left(\frac{\mathbf{r}}{Q} \right)_t = \mathbf{E}(\mathbf{r}) \mathbf{r}_t,$$

we have

$$\begin{aligned} & \int_K \frac{1}{2} H^2 Q_t dK + \int_K Q H H_t dK + \int_K \frac{(u_t)^2}{Q} dK \\ & - \int_K \nabla \cdot ((\mathbf{s} - \mathbf{v}) u_t) + \int_{\partial K} (\widehat{\mathbf{s}} \cdot \boldsymbol{\nu} - \widehat{\mathbf{v}} \cdot \boldsymbol{\nu}) u_t ds + \int_{\partial K} \widehat{u}_t \boldsymbol{\nu} \cdot (\mathbf{s} - \mathbf{v}) ds \\ & + \int_K \nabla \cdot (\mathbf{q}_t W) dK - \int_{\partial K} \widehat{\mathbf{q}_t} \cdot \boldsymbol{\nu} W ds - \int_{\partial K} \widehat{W} \boldsymbol{\nu} \cdot \mathbf{q}_t ds = 0. \end{aligned}$$

Summing up over K , with the numerical fluxes (3.5) and the periodic boundary conditions, we get

$$\int_{\Omega} \frac{1}{2} H^2 Q_t d\Omega + \int_{\Omega} Q H H_t d\Omega + \int_{\Omega} \frac{(u_t)^2}{Q} d\Omega = 0,$$

i.e.

$$\frac{1}{2} \frac{d}{dt} \int_{\Omega} H^2 Q d\Omega + \int_{\Omega} \frac{(u_t)^2}{Q} d\Omega = 0.$$

□

4 Numerical results

In this section we provide numerical examples to illustrate the accuracy and capability of the LDG method. Time discretization is by the forward Euler method with a suitably small Δt for stability. Since $\Delta t = O(h^4)$ for the stability constraint, accuracy is maintained up to fourth order. This is not the most efficient method for the time discretization to our LDG scheme. However, we will not address the issue of time discretization efficiency in this paper. For all the numerical simulation presented in this section, domain with periodic boundary conditions are considered. We have verified with the aid of successive mesh refinements, that in all cases, the results shown are numerically convergent.

4.1 Surface diffusion of graphs

In this section, we consider numerical simulation for surface diffusion of graphs

$$u_t + \nabla \cdot \left(Q \left(\mathbf{I} - \frac{\nabla u \otimes \nabla u}{Q^2} \right) \nabla H \right) = 0, \quad (4.1)$$

where Q and H are defined by (1.3) and (1.4).

Example 4.1. Accuracy test

In this example, we consider the accuracy test for one-dimensional surface diffusion of graphs. We test our method taking the exact solution

$$u(x, t) = 0.05 \sin(x) \cos(t) \quad (4.2)$$

for the surface diffusion of graphs equation with a source term f , which is a given function so that (4.2) is the exact solution. The computational domain is $[-\pi, \pi]$. The

Table 4.1: Accuracy test for one-dimensional surface diffusion of graphs with the exact solution (4.2). Uniform meshes with J cells at time $t = 0.5$.

	J	L^∞ error	order	L^2 error	order
P^0	10	5.93E-03	–	1.37E-02	–
	20	2.95E-03	1.00	6.88E-03	0.99
	40	1.48E-03	1.00	3.45E-03	1.00
	80	7.38E-04	1.00	1.72E-03	1.00
P^1	10	8.00E-04	–	2.86E-03	–
	20	1.99E-04	2.00	7.17E-04	2.00
	40	4.98E-05	2.00	1.80E-04	1.99
	80	1.25E-05	2.00	4.51E-05	2.00
P^2	10	4.24E-05	–	1.76E-04	–
	20	5.29E-06	3.00	2.25E-05	2.96
	40	6.62E-07	3.00	2.83E-06	2.99
	80	8.75E-08	2.92	3.75E-07	2.92

L^2 and L^∞ errors and the numerical orders of accuracy at time $t = 0.5$ with uniform meshes are contained in Table 4.1. We can see that the method with P^k elements gives $(k+1)$ -th order of accuracy in both L^2 and L^∞ norms.

Example 4.2. Positive perturbation

In this example, we consider the numerical solutions of the two-dimensional surface diffusion of graphs equation (4.1) with the initial condition

$$u_0(x, y) = 1 + 0.3 \min(1, \max(0, 2 - 5\sqrt{x^2 + y^2})). \quad (4.3)$$

The computational domain is $[-1, 1]$. We use P^2 elements with 40×40 uniform rectangular cells in our computation of the LDG method. The solutions at time $t = 0, 0.0001, 0.001$ and 0.005 are shown in Figure 4.1. Even if we use a coarse mesh, we still obtain a good resolution of the solution comparable with that in [1]. We also observe similar phenomena as in [1]: a strong smoothing effect much faster for high frequencies

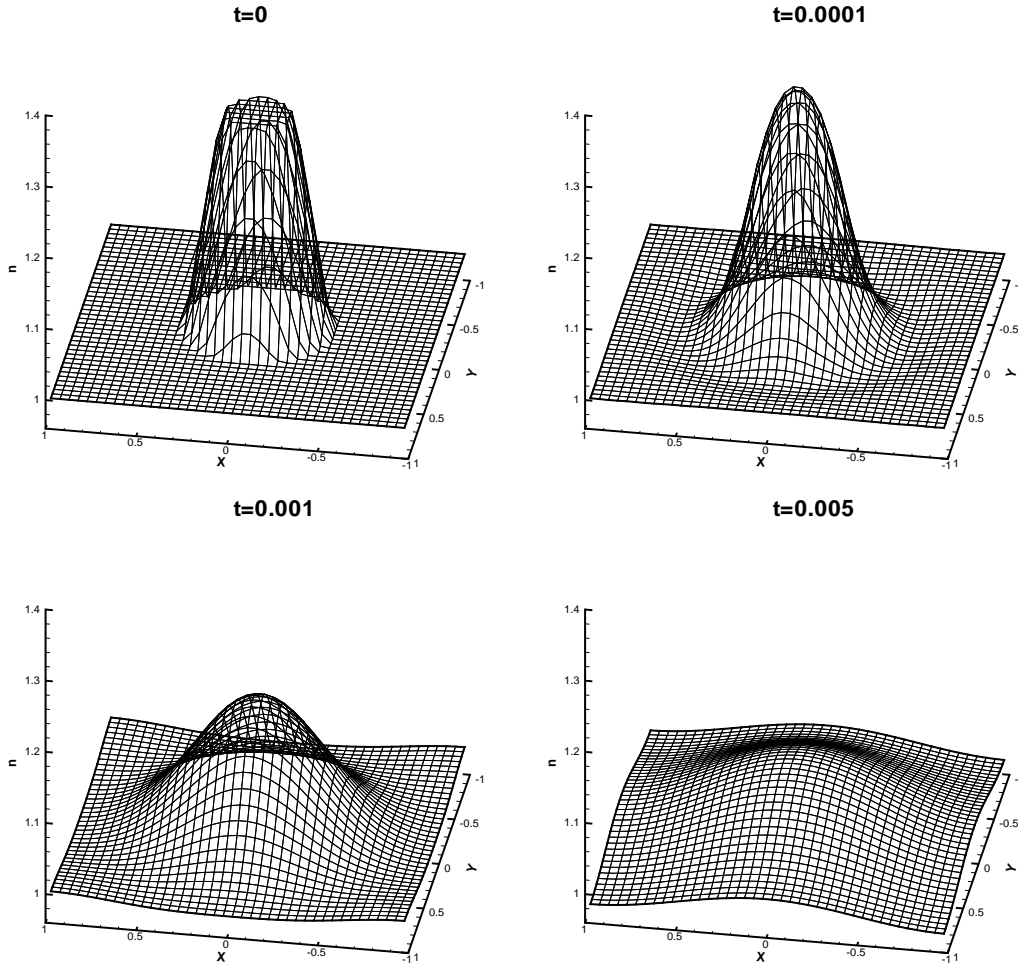


Figure 4.1: The solution with positive perturbation of the surface diffusion of graphs equation (4.1) with the initial condition (4.3). Periodic boundary condition in $[-1, 1]$. P^2 elements and a uniform mesh with 40×40 cells.

than for low frequencies, as well as the solution becoming less than 1 (lack of maximum principle).

Example 4.3. Sine perturbation

In this example, we consider the numerical solutions of the two-dimensional surface diffusion of graphs equation (4.1) with the initial condition

$$u_0(x, y) = 1 - 0.1 \sin(\pi x) \sin(\pi y). \quad (4.4)$$

The computational domain is $[-1, 1]$. We use P^2 elements with 40×40 cells in our computation of the LDG method. The graph evolution at time $t = 0, 0.001, 0.005$ and

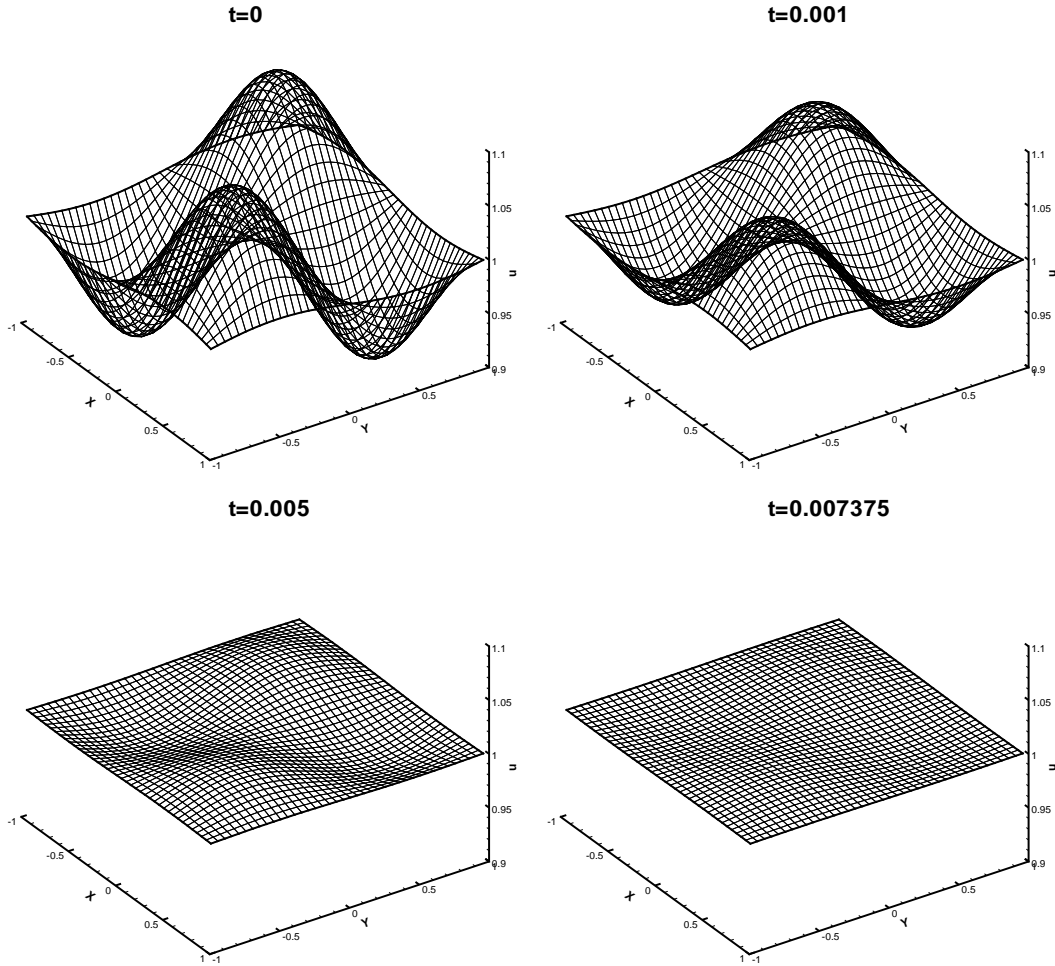


Figure 4.2: The solution of the surface diffusion of graphs equation (4.1) with the initial condition (4.4). Periodic boundary condition in $[-1, 1]$. P^2 elements and a uniform mesh with 40×40 cells.

0.007375 is illustrated in Figure 4.2. Smoothing effect is very obvious as in Example 4.2.

Example 4.4. Perturbation with superposition of sines

In this example, we consider numerical solutions of the two-dimensional surface diffusion of graphs equation (4.1) with the initial condition

$$u_0(x, y) = 1 + 0.1 \sin(\pi(x + y)) + 0.3 \sin(4\pi(x + y)). \quad (4.5)$$

The computational domain is $[-1, 1]$. We use P^2 elements with 40×40 cells in our computation of the LDG method. The solutions at time $t = 0, 0.0001, 0.001$ and

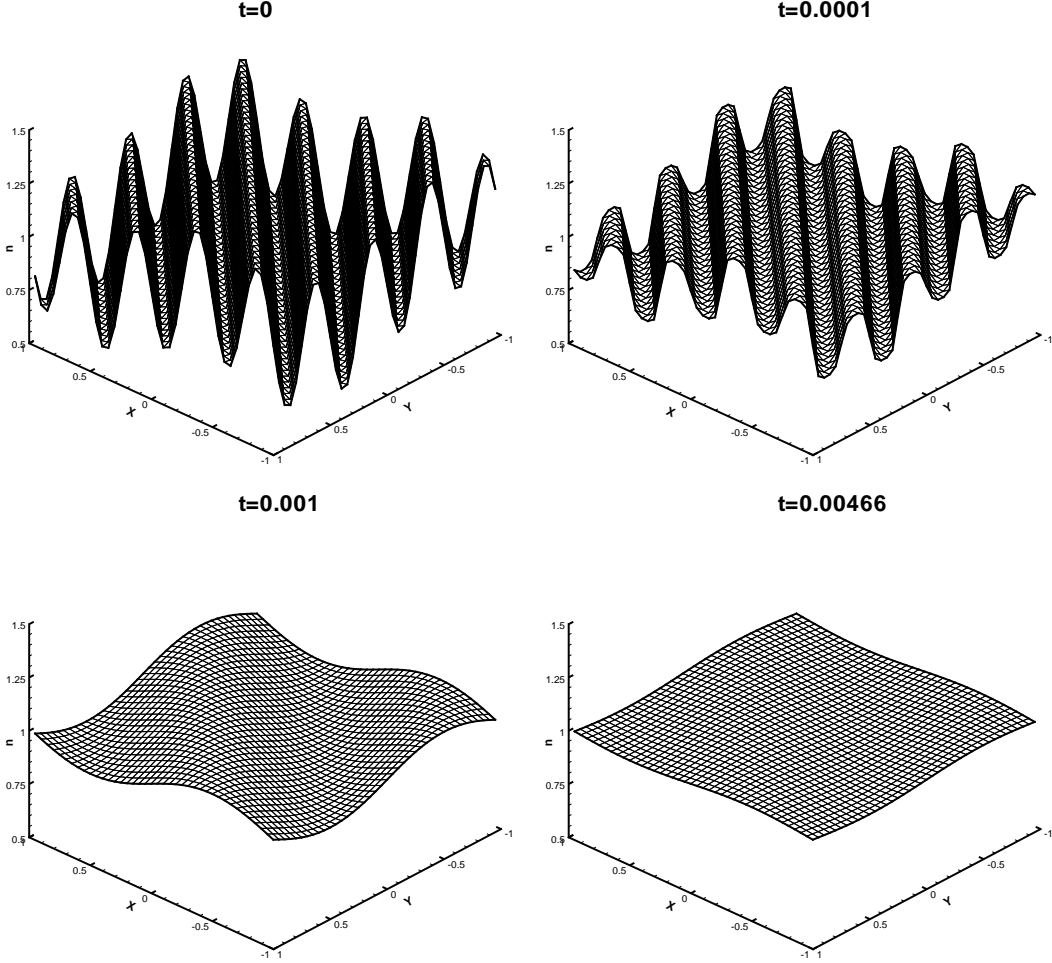


Figure 4.3: The solution of the surface diffusion of graphs equation (4.1) with the initial condition (4.5). Periodic boundary condition in $[-1, 1]$. P^2 elements and a uniform mesh with 40×40 cells.

0.00466 are shown in Figure 4.2. The results show that high frequencies are rapidly damped and the amplitude of low frequency waves decays very slowly.

4.2 Willmore flow of graphs

In this section, we consider numerical simulation for the Willmore flow of graphs

$$u_t + Q \nabla \cdot \left(\frac{1}{Q} \left(\mathbf{I} - \frac{\nabla u \otimes \nabla u}{Q^2} \right) \nabla(QH) \right) - \frac{1}{2} Q \nabla \cdot \left(\frac{H^2}{Q} \nabla u \right) = 0, \quad (4.6)$$

where Q and H are defined by (1.3) and (1.4).

Example 4.5. Accuracy test

Table 4.2: Accuracy test for one-dimensional surface diffusion of graphs with the exact solution (4.2). Uniform meshes with J cells at time $t = 0.5$.

	J	L^∞ error	order	L^2 error	order
P^0	10	1.17E-02	–	2.73E-02	–
	20	5.89E-03	0.99	1.37E-02	0.99
	40	2.95E-03	1.00	6.89E-03	1.00
	80	1.47E-03	1.00	3.45E-03	1.00
P^1	10	2.83E-03	–	1.03E-02	–
	20	7.23E-04	1.97	2.66E-03	1.96
	40	1.81E-04	2.00	6.70E-04	1.99
	80	4.41E-05	2.04	1.65E-04	2.02
P^2	10	4.74E-04	–	1.95E-03	–
	20	5.97E-05	2.99	2.51E-04	2.95
	40	7.83E-06	2.93	3.15E-05	3.00
	80	1.05E-06	2.90	4.07E-06	2.95

In this example, we consider the accuracy test for one-dimensional Willmore flow of graphs. We test our method taking the exact solution

$$u(x, t) = 0.05 \sin(x) \cos(t) \quad (4.7)$$

for the Willmore flow of graphs equation with a source term f chosen as a given function so that (4.7) is the exact solution. The L^2 and L^∞ errors and the numerical orders of accuracy at time $t = 0.5$ with uniform meshes are contained in Table 4.2. The computational domain is $[-\pi, \pi]$. We can see that the method with P^k elements gives $(k+1)$ -th order of accuracy in both L^2 and L^∞ norms.

Example 4.6. Perturbation with superposition of sines

In this example, we consider the numerical solutions of the two-dimensional Willmore flow of graphs equation (4.6) with the initial condition

$$u_0(x, y) = 0.75 \sin^2(\pi(1 + x)) \sin^2(\pi x) + 0.1 \sin(4\pi x) \sin(5\pi y) \quad (4.8)$$

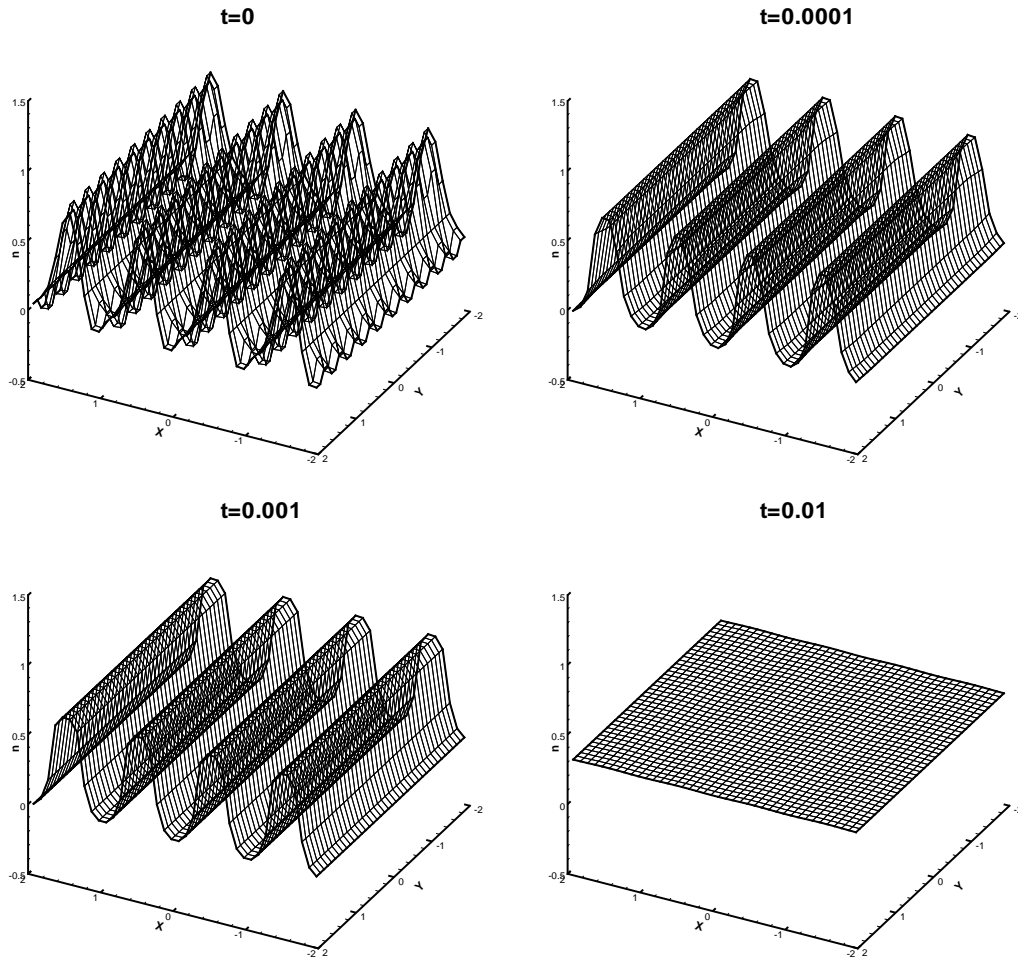


Figure 4.4: The solution of the Willmore flow of graphs equation (4.6) with the initial condition (4.8). Periodic boundary condition in $[-2, 2]$. P^2 elements and a uniform mesh with 40×40 cells.

The computational domain is $[-2, 2]$. We use P^2 elements with 40×40 cells in our computation of the LDG method. The solutions at time $t = 0, 0.0001, 0.001$ and 0.01 are shown in Figure 4.4. Similar smoothing effect as the surface diffusion of graphs equation are observed and the numerical solutions are being damped very rapidly.

Example 4.7. Convergence towards the planar surface

In this example, we consider the numerical solutions of the two-dimensional Willmore flow of graphs equation (4.6) with the initial condition

$$u_0(x, y) = \frac{1}{2} \sin \left(\pi \tanh \left(5(x^2 + y^2) - \frac{1}{4} \right) \right) \quad (4.9)$$

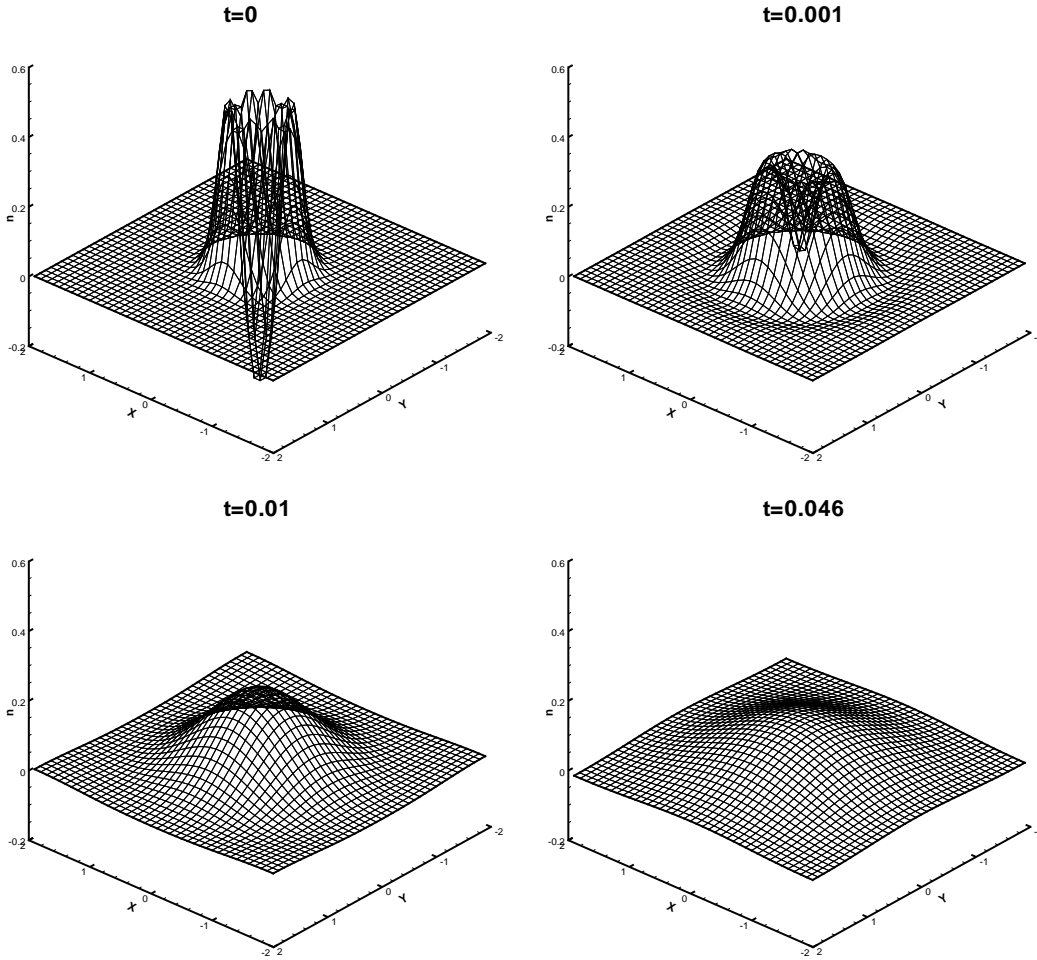


Figure 4.5: The solution of the Willmore flow of graphs equation (4.6) with the initial condition (4.9). Periodic boundary condition in $[-2, 2]$. P^2 elements and a uniform mesh with 40×40 cells.

The computational domain is $[-2, 2]$. We use P^2 elements with 40×40 cells in our computation of the LDG method. The solutions at time $t = 0, 0.001, 0.01$ and 0.046 are shown in Figure 4.5. A strong smoothing effect is much faster for high frequencies than for low frequencies. High frequencies are rapidly damped.

Example 4.8. Sine perturbation

In this example, we consider the numerical solutions of the two-dimensional Willmore flow of graphs equation (4.6) with the initial condition

$$u_0(x, y) = 0.25 \sin(\pi y)(0.25 \sin(\pi x) + 0.5 \sin(3\pi x)) \quad (4.10)$$

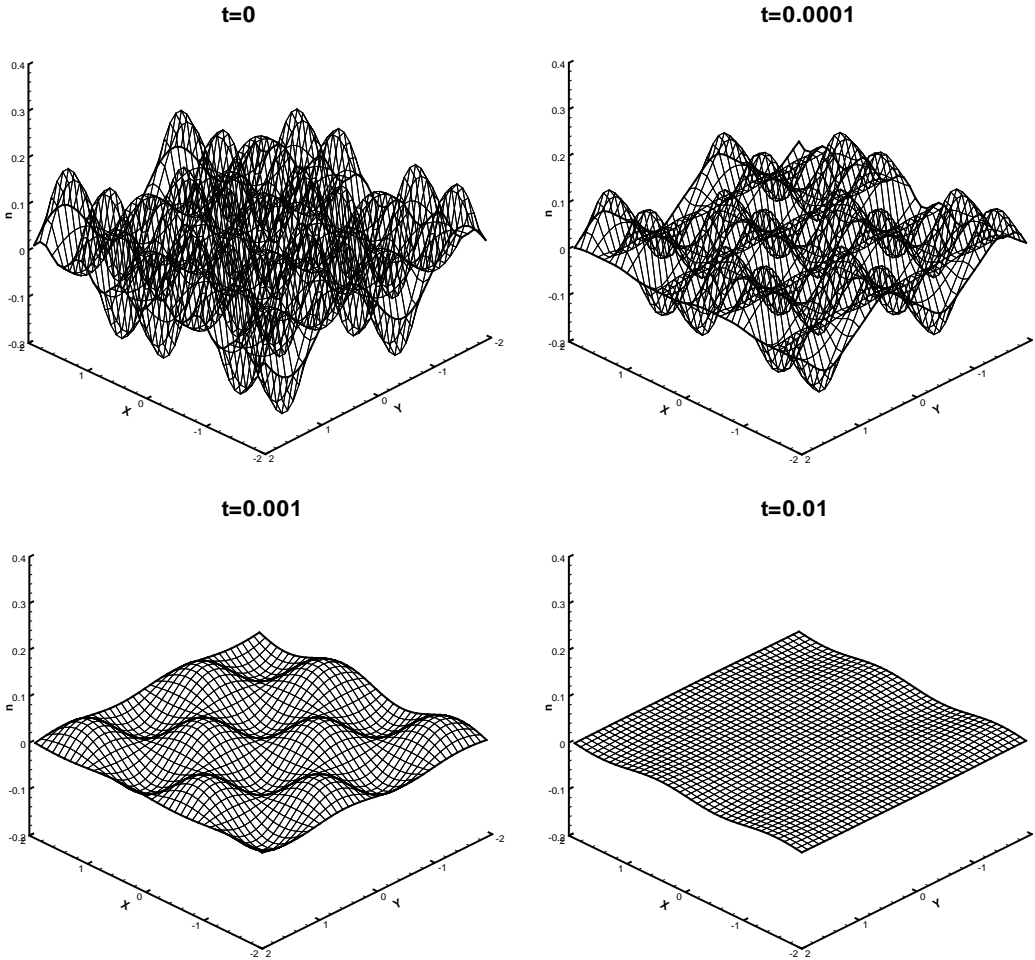


Figure 4.6: The solution of the Willmore flow of graphs equation (4.6) with the initial condition (4.10). Periodic boundary condition in $[-2, 2]$. P^2 elements and a uniform mesh with 40×40 cells.

The computational domain is $[-2, 2]$. We use P^2 elements with 40×40 cells in our computation of the LDG method. The solutions at time $t = 0, 0.0001, 0.001$ and 0.01 are shown in Figure 4.6. The results show that high frequencies are rapidly damped and the amplitude of the waves decays very fast.

5 Conclusion

We have developed a local discontinuous Galerkin method to solve the surface diffusion of graphs and Willmore flow of graphs equations. L^2 stability and energy stability are

proven for general solutions. Numerical examples are given to illustrate the accuracy and capability of the methods. Although not addressed in this paper, the LDG methods are flexible for general geometry, unstructured meshes and h - p adaptivity. That will be our future work on solving nonlinear equations in geometric partial differential equations.

References

- [1] E. Bänsch, P. Morin and R.H. Nochetto, *Surface diffusion of graphs: variational formulation, error analysis, and simulation*, SIAM J. Numer. Anal., **42** (2004), pp.773-799.
- [2] F. Bassi and S. Rebay, *A high-order accurate discontinuous finite element method for the numerical solution of the compressible Navier-Stokes equations*, J. Comput. Phys., **131** (1997), pp.267-279.
- [3] M. Beneš, *Numerical solution for surface diffusion on graphs*, Proceedings of Czech-Japanese Seminar in Applied Mathematics 2005, COE Lect. Note, 3, Kyushu Univ. The 21 Century COE Program, Fukuoka, 2006, pp.9-25.
- [4] B. Cockburn, *Discontinuous Galerkin methods for methods for convection-dominated problems*, in *High-Order Methods for Computational Physics*, T.J. Barth and H. Deconinck, editors, Lecture Notes in Computational Science and Engineering, volume 9, Springer, 1999, pp.69-224.
- [5] B. Cockburn, S. Hou and C.-W. Shu, *The Runge-Kutta local projection discontinuous Galerkin finite element method for conservation laws IV: the multidimensional case*, Math. Comp., **54** (1990), pp.545-581.
- [6] B. Cockburn, S.-Y. Lin and C.-W. Shu, *TVB Runge-Kutta local projection discontinuous Galerkin finite element method for conservation laws III: one dimensional systems*, J. Comput. Phys., **84** (1989), pp.90-113.

- [7] B. Cockburn and C.-W. Shu, *TVB Runge-Kutta local projection discontinuous Galerkin finite element method for conservation laws II: general framework*, Math. Comp., **52** (1989), pp.411-435.
- [8] B. Cockburn and C.-W. Shu, *The Runge-Kutta discontinuous Galerkin method for conservation laws V: multidimensional systems*, J. Comput. Phys., **141** (1998), pp.199-224.
- [9] B. Cockburn and C.-W. Shu, *The local discontinuous Galerkin method for time-dependent convection-diffusion systems*, SIAM J. Numer. Anal., **35** (1998), pp.2440-2463.
- [10] B. Cockburn and C.-W. Shu, *Runge-Kutta Discontinuous Galerkin methods for convection-dominated problems*, J. Sci. Comput., **16** (2001), pp.173-261.
- [11] B. Cockburn and C.-W. Shu, *Foreword for the special issue on discontinuous Galerkin method*, J. Sci. Comput., **22-23** (2005), pp.1-3.
- [12] B. Coleman, R. Falk and M. Moakher, *Space-time finite element methods for surface diffusion with applications to the theory of the stability of cylinders*, SIAM J. Sci. Comput., **17** (1996), pp.1434-1448.
- [13] C. Dawson, *Foreword for the special issue on discontinuous Galerkin method*, Comput. Meth. Appl. Mech. Engrg., **195** (2006), p.3183.
- [14] K. Deckelnick, G. Dziuk and C.M. Elliott, *Computation of geometric partial differential equations and mean curvature flow*, Acta Numer., **14** (2005), pp.139-232.
- [15] K. Deckelnick and G. Dziuk, *Error analysis of a finite element method for the Willmore flow of graphs*, Interfaces Free Bound., **8** (2006), pp.21-46.
- [16] M. Droske and M. Rumpf, *A level set formulation for Willmore flow*, Interfaces and Free Bound., **6** (2004), pp.361-378.

- [17] Q. Du, C. Liu and X. Wang, *A phase field approach in the numerical study of the elastic bending energy for vesicle membranes*, J. Comput. Phys., **198** (2004), pp.450-468.
- [18] Q. Du, C. Liu, R. Ryham and X. Wang, *A phase field formulation of the Willmore problem*, Nonlinearity, **18** (2005), pp.1249-1267.
- [19] G. Dziuk, E. Kuwert and R. Schätzle, *Evolution of elastic curves in \mathbb{R}^n : existence and computation*, SIAM J. Math. Anal., **33** (2002), pp.1228-1245.
- [20] W.H. Reed and T.R. Hill, *Triangular mesh method for the neutron transport equation*, Technical report LA-UR-73-479, Los Alamos Scientific Laboratory, Los Alamos, NM, 1973.
- [21] T. Oberhuber, *Numerical solution for the Willmore flow of graphs*, Proceedings of Czech-Japanese Seminar in Applied Mathematics 2005, COE Lect. Note, 3, Kyushu Univ. The 21 Century COE Program, Fukuoka, 2006, pp.126-138.
- [22] Y. Xia, Y. Xu and C.-W. Shu, *Local discontinuous Galerkin methods for the Cahn-Hilliard type equations*, J. Comput. Phys., **227** (2007), pp. 472-491.
- [23] Y. Xia, Y. Xu and C.-W. Shu, *Application of the local discontinuous Galerkin method for the Allen-Cahn/Cahn-Hilliard system*, Communications in Computational Physics, to appear.
- [24] Y. Xu and C.-W. Shu, *Local discontinuous Galerkin methods for nonlinear Schrödinger equations*, J. Comput. Phys., **205** (2005), pp.72-97.
- [25] Y. Xu and C.-W. Shu, *Local discontinuous Galerkin methods for two classes of two dimensional nonlinear wave equations*, Physica D, **208** (2005), pp.21-58.
- [26] J. Yan and C.-W. Shu, *A local discontinuous Galerkin method for KdV type equations*, SIAM J. Numer. Anal., **40** (2002), pp.769-791.